

Cell Reports, Volume 28

Supplemental Information

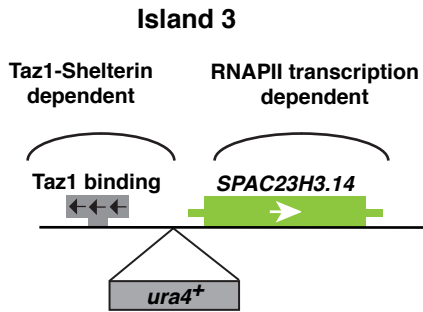
CPF Recruitment to Non-canonical

Transcription Termination Sites Triggers

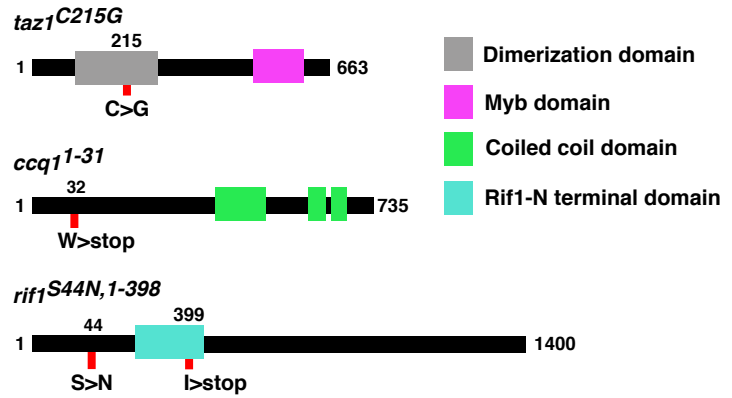
Heterochromatin Assembly and Gene Silencing

Tommy V. Vo, Jothy Dhakshnamoorthy, Madeline Larkin, Martin Zofall, Gobi Thillainadesan, Vanivilasini Balachandran, Sahana Holla, David Wheeler, and Shiv I.S. Grewal

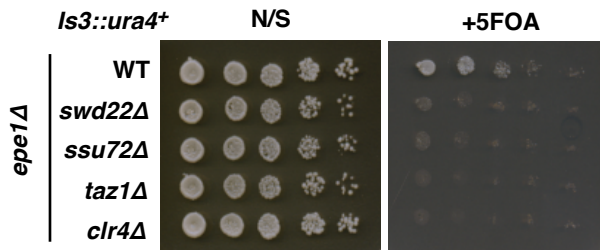
A



B



C



D

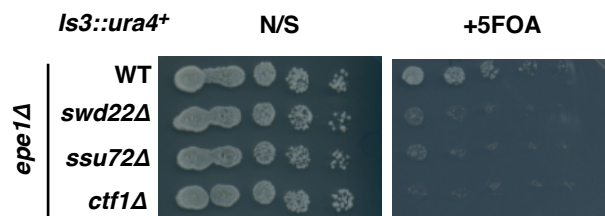


Figure S1. Identification of factors required for RNAi-independent heterochromatic silencing, Related to Figure 1.

(A) Diagram showing the chromosomal region containing Island 3. In addition to harboring binding sites for Shelterin subunit Taz1 which nucleates heterochromatin by recruiting Clr4 (Zofall et al., 2016), RNAPII transcription-dependent mechanism(s) trigger H3K9me at the *SPAC23H3.14* locus (Reyes-Turcu et al., 2011). (B) Graphical representation of Taz1, Ccq1 and Rif1 protein domains. The locations of mutations identified from the genetic screen are indicated by red rectangles. (C and D) Serial dilution spotting analyses to assay for expression of *Is3::ura4+* in the indicated strains. Expression of *Is3::ura4+* leads to growth defects on +5FOA medium. Also shown is growth on non-selective medium (N/S).

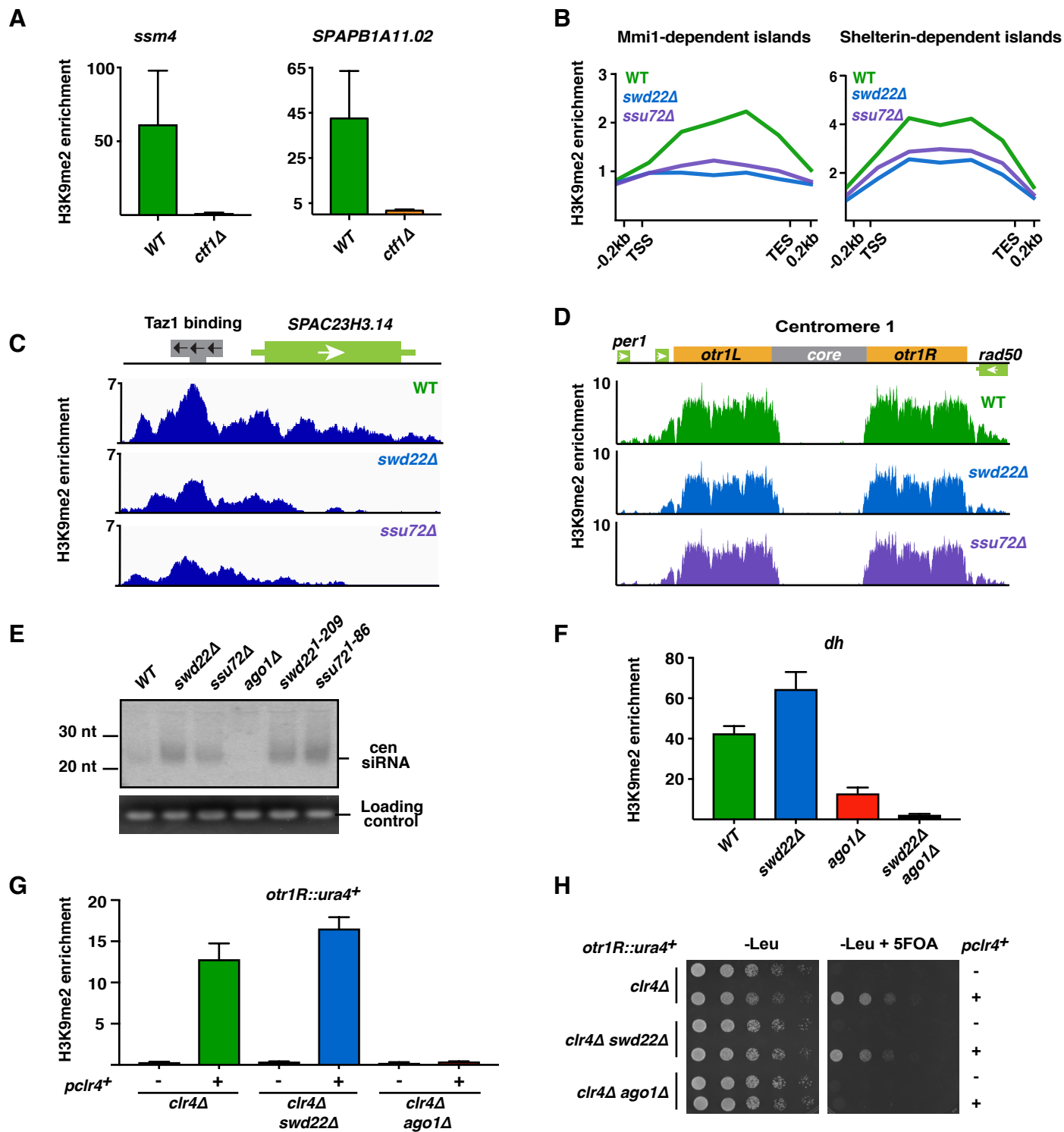


Figure S2. CPF contributes to assembly of facultative and constitutive heterochromatin, Related to Figure 2.

(A) ChIP-qPCR analyses of H3K9me2 fold enrichment at *ssm4* and *SPAPB1A11.02* loci relative to the control *leu1* gene. N=3, error bars shown are SD. (B) Median H3K9me2 enrichment at Mmi1-dependent and Shelterin-dependent islands. Islands are listed in Table S1. TSS, transcription start site; TES, transcription end site. (C) ChIP-seq H3K9me2 enrichment at Island 3 in cells grown at 18°C. (D) H3K9me2 enrichment at *cen1*. Enrichment is the ratio of immunoprecipitated chromatin over whole-cell extract and is shown as reads per genomic content (RPGC). (E) Northern blot probe for centromeric siRNAs. (F) H3K9me2 enrichment at pericentromeric *dh* repeats relative to *act1* gene. N=3, error bars are SD. (G) H3K9me2 enrichment at *otr1R::ura4+* relative to the control *leu1* gene, based on ChIP-qPCR analysis. N = 2, error bars are SD. (H) Serial dilution spotting assay to measure *otr1R::ura4+* expression. Plasmids were maintained in -Leu medium. Cells with silenced *otr1R::ura4+* grow on +5FOA medium.

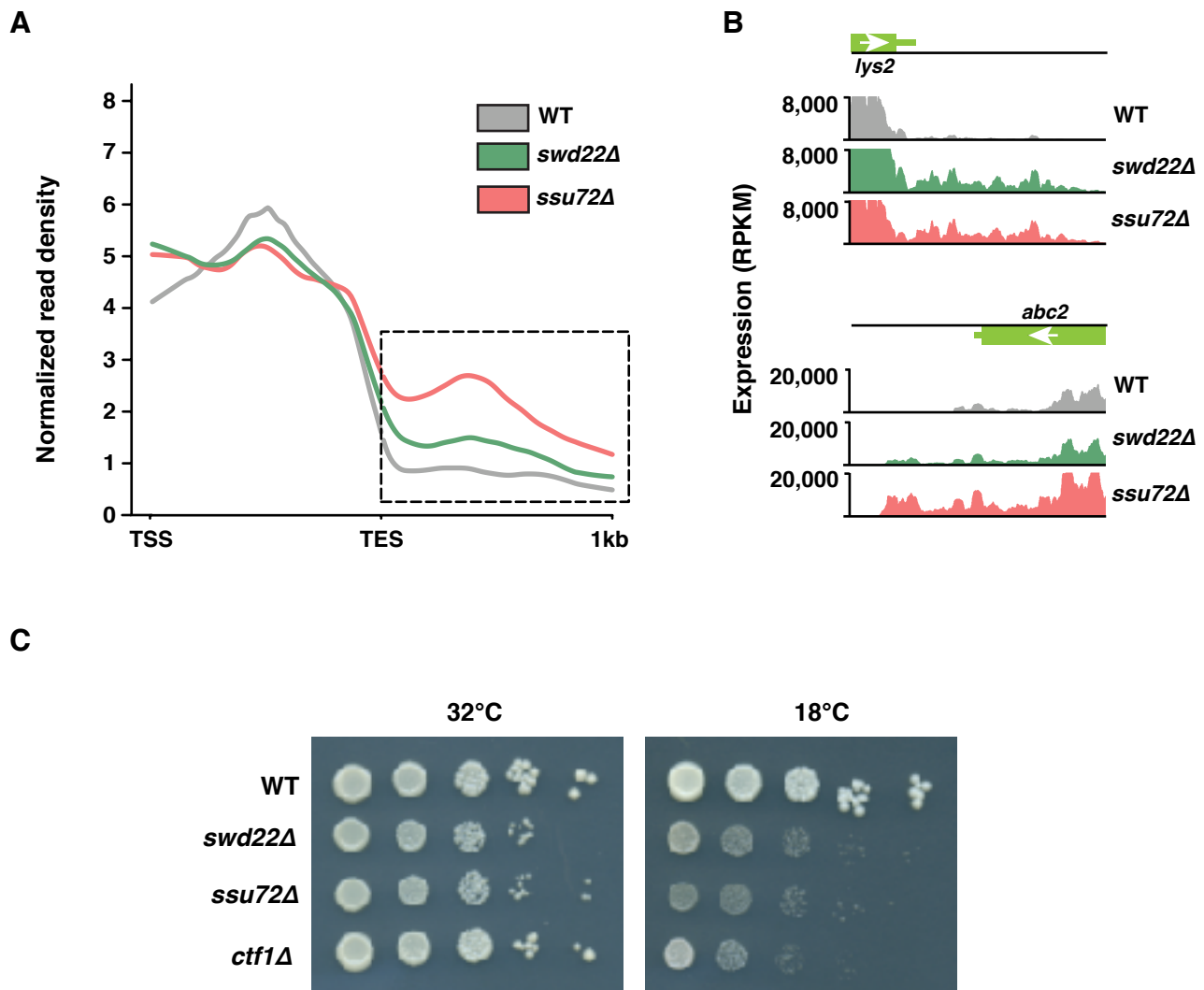


Figure S3. CPF is required for preventing readthrough transcription and cold sensitivity, Related to Figure 3.

(A) RNA-seq read-depth is plotted for the gene body and downstream region of 25 transcripts that show elevated downstream transcription in CPF deletion strains. TSS, transcription start site; TES, transcription end site. The read-depths for each mutant strain are normalized to the mean depth within the wild type gene body to correct for differences in the expression of the upstream transcript. Depth is normalized to reads-per-million (RPM). (B) RNA-seq profiles showing read through transcription at the representative loci *lys2* and *abc2* in CPF deletion strains. (C) Serial dilutions of WT and deletion strains were spotted on rich medium and assayed for growth at normal and low temperature.

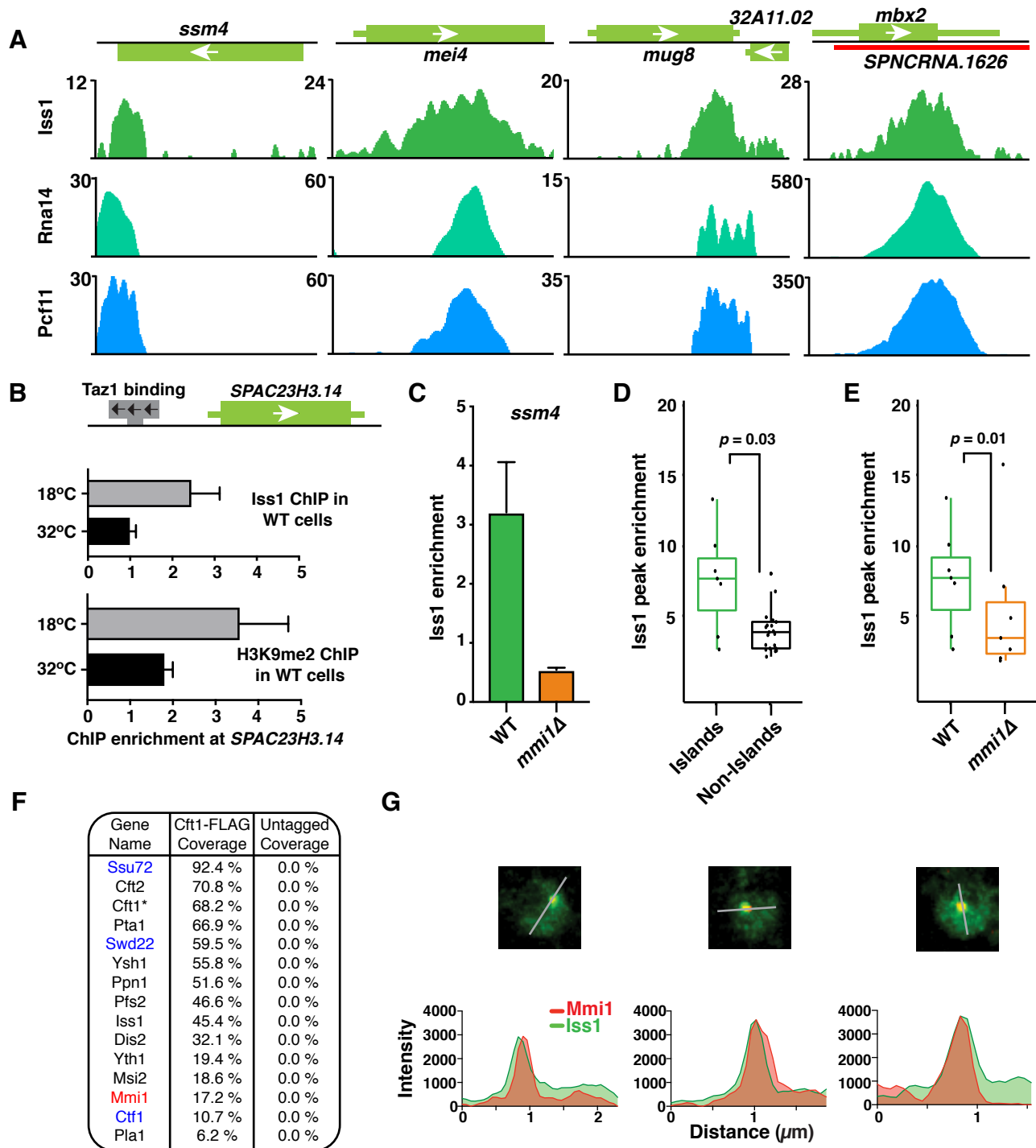


Figure S4. CPF is enriched preferentially at Mmi1-dependent meiotic facultative heterochromatin islands, Related to Figure 4.

(A) Distribution of CPF core and accessory subunits at meiotic facultative heterochromatin islands as assessed by ChIP-seq analyses. Iss1 plots are also shown in Figure 4A. Rna14 and Pcf11 ChIP-seq data were replotted from Laroche et al., 2018. Enrichment values shown represent the subtraction of whole-cell extract from immunoprecipitated chromatin. (B) Iss1 and H3K9me2 ChIP-qPCR analyses in WT at island 3 at 18°C or 32°C. Enrichments at *SPAC23H3.14* relative to the control *leu1* gene. N=3, error bars shown are SD. (C) ChIP-qPCR enrichment analysis of core CPF subunit Iss1 at *ssm4* locus relative to the control *leu1* gene. N=3, error bars shown are SD. (D) Box plot of Iss1 peak signals at island Mmi1 regulon genes (N=7) and non-island Mmi1 regulon genes (N=21) in WT cells. Statistical analysis used the Wilcoxon rank sum test. (E) Box plot of Iss1 peaks at island Mmi1 regulon genes (N=7) in WT and *mmi1* deletion cells. Statistical analysis used Wilcoxon signed rank test. For all box plots, median 99th percentile signal in the gene CDS were compared; individual genes are denoted by black dots. Island and non-island Mmi1 regulon genes are listed in Table S3. (F) FLAG-tagged core CPF subunit Cft1(*) copurified with other known components of the CPF complex and Mmi1 (red). Shown are protein coverage percentages in tagged and untagged purifications. Relevant proteins associating with Cft1 are shown. Mutations in Ssu72, Swd22, and Ctf1 subunits (highlighted in blue) cause defects in heterochromatin assembly (Figures 2 and S2). (G) Line plot profiles of three representative cells highlighted in Figure 4F. Profiles show the distribution of fluorescent signals across each cell. Gray bar denotes the axis of quantification.

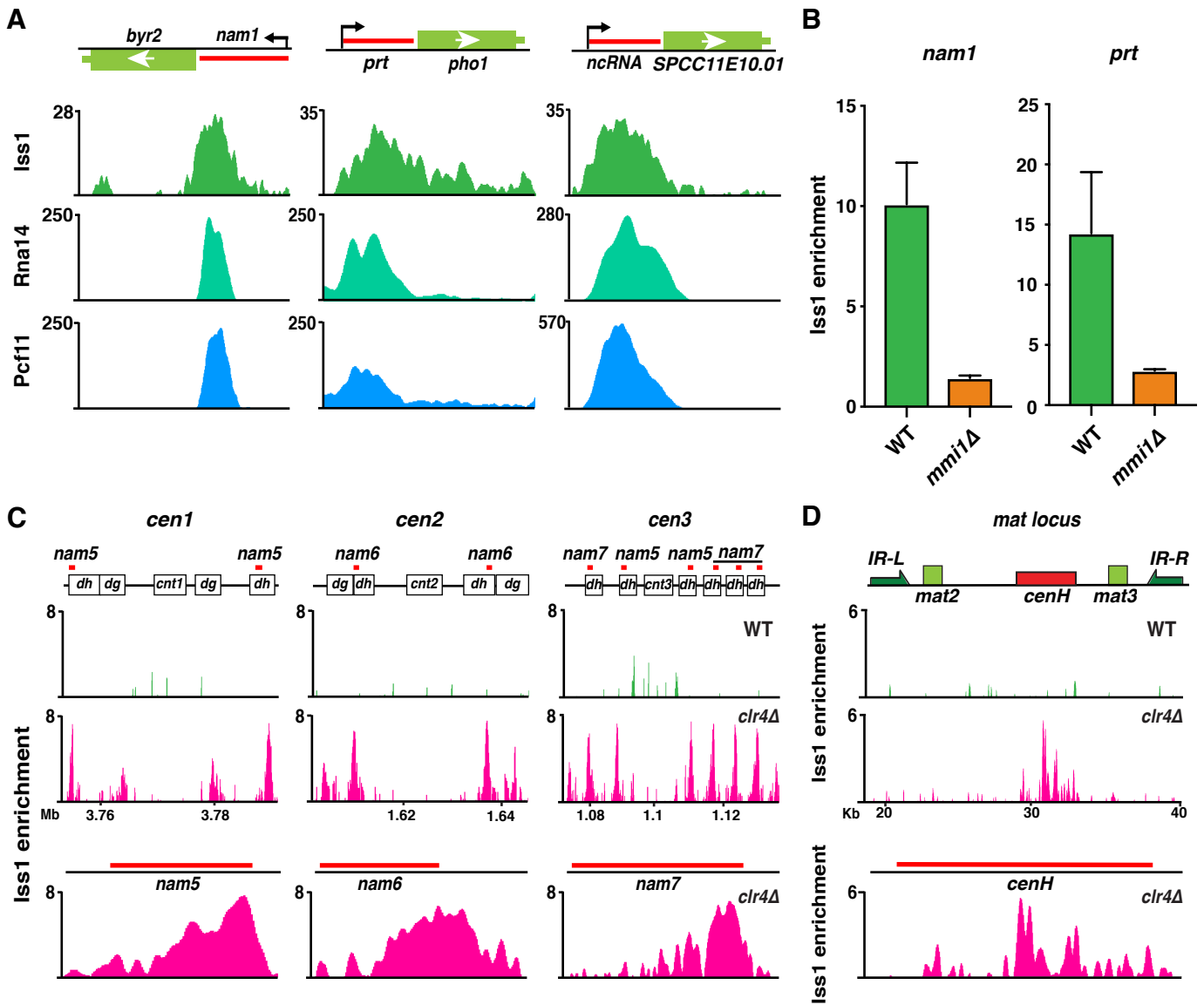


Figure S5. CPF localizes to lncRNAs targeted by Mmi1, Related to Figure 5.

(A) Distribution of CPF core and accessory subunits Iss1, Rna14, and Pcf11 at lncRNAs (red line) adjacent to *byr2*, *pho1*, and *SPCC11E10.01* as determined by ChIP-seq analyses. Iss1 plots are also shown in Figure 5A. Rna14 and Pcf11 ChIP-seq data were replotted from Larochelle et al., 2018. Enrichment values shown represent the subtraction of whole-cell extract from immunoprecipitated chromatin. (B) ChIP-qPCR enrichment analyses of Iss1 at lncRNA loci *nam1* and *prt* relative to the control *leu1* gene. N=3, error bars shown are SD. (C) Iss1 enrichment at the centromeres in WT or *clr4* deletion cells. Annotated *nam5/6/7* lncRNAs previously identified in Touat-Todeschini et al., 2017 are depicted. Iss1 enrichment at individual *nam* lncRNAs in *clr4* deletion cells is depicted below. (D) Iss1 enrichment at the mating type locus in WT or *clr4* deletion cells. Iss1 enrichment at the *cenH* locus in *clr4* deletion cells is shown below.

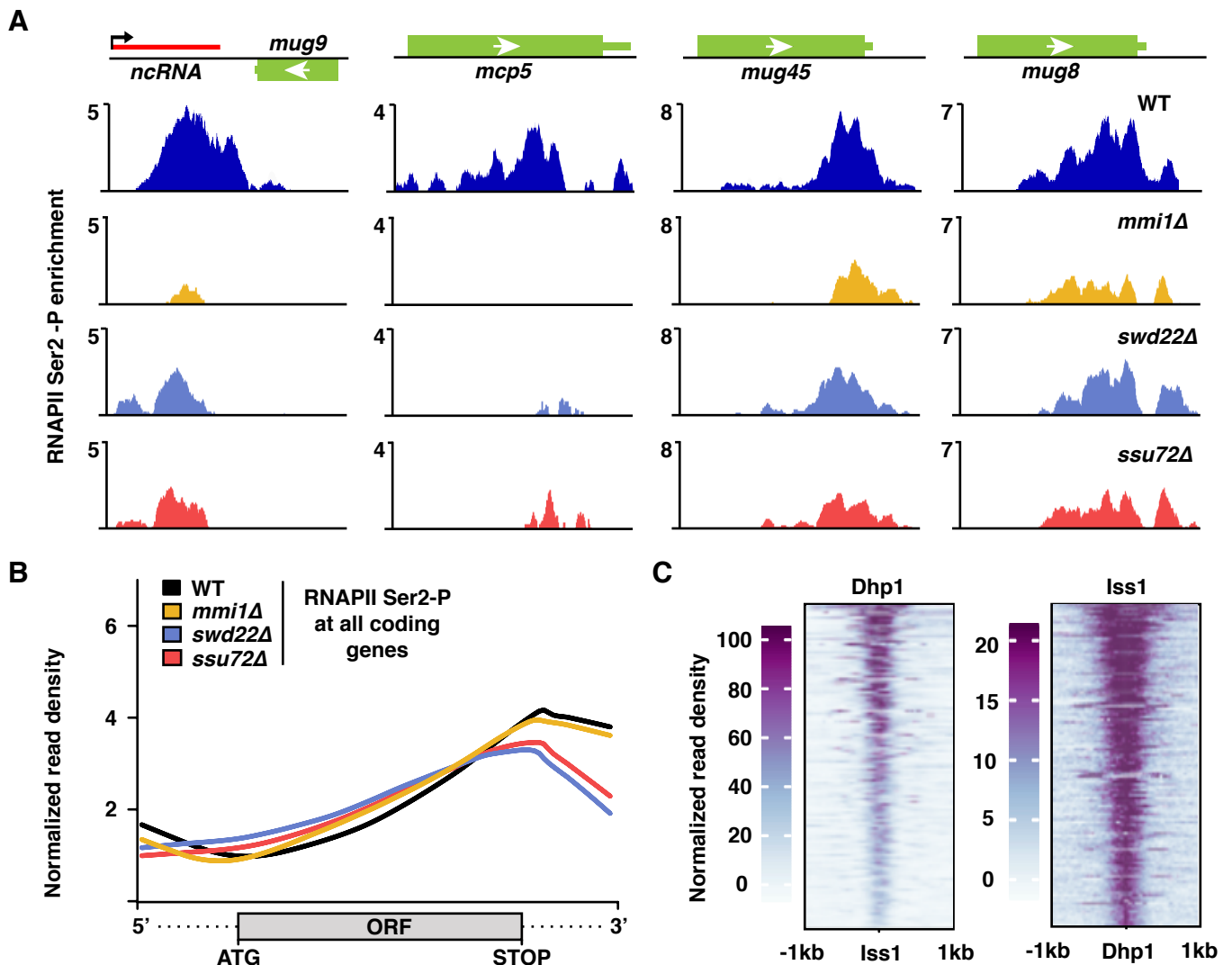


Figure S6. CPF is required for RNAPII Ser2-P pileups at Mmi1 target loci, Related to Figure 6.

(A) ChIP-seq analyses of RNAPII Ser2-P pileup at *mug9*, *mcp5*, *mug45*, and *mug8* in WT and deletion strains. Enrichment values shown represent the subtraction of whole-cell extract from immunoprecipitated chromatin. (B) Median RNAPII Ser2-P enrichment in WT or deletion strains across all coding genes (N = 5,144) based on ChIP-seq analyses. (C) (Left) Heatmap of Dhp1 enrichment plotted over a 2 kb window centered on the locations of each Iss1 peak (N=344). Each row represents a 2 kb region centered on an Iss1 peak and are sorted from highest to lowest overall Dhp1 enrichment. (Right) Heatmap of Iss1 enrichment plotted over a 2 kb window centered on the locations of each Dhp1 peak (N=958). Each row represents a 2 kb region and are sorted from highest to lowest overall Iss1 enrichment.

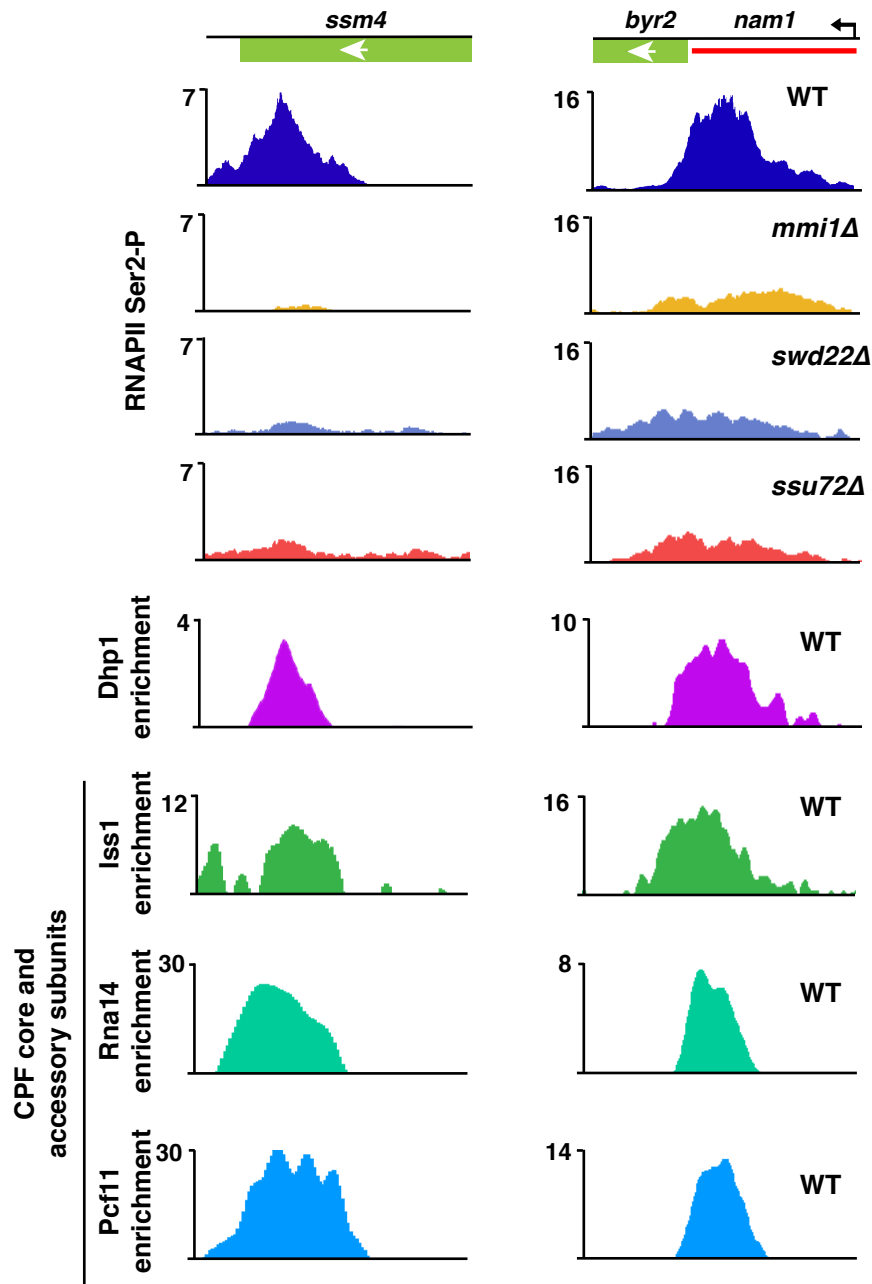


Figure S7. Composite figure showing colocalization of RNAPII Ser2-P and transcription termination factors at a meiotic gene and lncRNA locus, Related to Figure 7.

Distribution profiles of RNAPII Ser2-P, Dhp1, and CPF core and accessory subunits at representative loci corresponding to meiotic facultative heterochromatin (*ssm4*) and lncRNA (*nam1*) as assessed by ChIP-seq. Rna14 and Pcf11 ChIP-seq data were replotted from Larochelle et al., 2018.

Table S1. Effects of CPF mutants on H3K9me at 3 categories of heterochromatin islands. Related to Figure 2

Mmi1-dependent heterochromatin islands

Island number*	Genomic coordinates	Nearby gene	H3K9me2 WT	H3K9me2 <i>swd22Δ</i>	H3K9me2 <i>ssu72Δ</i>
1	I:578,438-581,236	<i>mcp7</i>	++	-	-
2	I:2,445,561-2,447,627	<i>mug8</i>	++	-	-
4	I:3,646,940-3,649,088	<i>spac8c9.04</i>	++++	+	-
5	I:3,727,304-3,729,052	<i>vps29</i>	++	-	-
6	I:4,533,508-4,536,707	<i>ssm4</i>	++++	-	+
8	II:898,362-901,026	<i>mcp5</i>	+	-	-
9	II:1,473,033-1,474,576	<i>mei4</i>	++++	-	+
16	II:3,626,236-3,628,856	<i>mbx2</i>	++	-	-
17	II:3639526-3640777	<i>mug45</i>	+	-	-
20	III:2,367,827-2,369,841	<i>mug9</i>	++	-	-

Shelterin-dependent heterochromatin islands

Island number*	Genomic coordinates	Nearby gene	H3K9me2 WT	H3K9me2 <i>swd22Δ</i>	H3K9me2 <i>ssu72Δ</i>
3	I:2,520,728-2,523,306	<i>spac23h3.14</i>	++	+	++
7	I:4,653,094-4,654,219	<i>spac144.02</i>	++++	++	++
13	II:1,868,149-1,868,769	<i>mug142</i>	++	+	++
14	II:2,198,013-2,200,240	<i>spncrna.394</i>	++++	+++	+++
15	II:2,338,199-2,341,250	<i>spbc24c6.09</i>	++++	++++	++++
19	III:1,037,820-1,039,129	<i>spcc1259.02c</i>	++++	+++	++++

Low temperature (18°C)-specific heterochromatin islands

Genomic coordinates	Nearby gene	H3K9me2 WT	H3K9me2 <i>swd22Δ</i>	H3K9me2 <i>ssu72Δ</i>
I:94,000-97,000	<i>isp3</i>	++	+	+
I:125,000-129,000	<i>SPAC11D3.10</i>	++	+	+
I:1,036,000-1,042,000	<i>SPAC23C4.05c</i>	+++	+	+
I:1,513,000-1,517,000	<i>ssz1</i>	++	+	+
I:2,147,000-2,150,000	<i>ala1</i>	+	-	-
I:2,174,000-2,179,000	<i>gld1</i>	++	-	+
I:2,395,000-2,398,500	<i>SPAC15F9.01c</i>	++	+	+
I:2,977,500-2,985,500	<i>SPAPB1A11.02</i>	+++	+	+
I:3,476,500-3,481,000	<i>tps1</i>	++++	+++	++++
I:5,309,000-5,311,500	<i>SPNCRNA.1069</i>	+	-	-
I:5,390,000-5,396,000	<i>SPAC3G6.07</i>	+++	+	++
II:102,000-105,000	<i>SPBC359.01</i>	+	-	+
II:167,500-170,500	<i>SPBC1683.12</i>	+	-	+

II:200,500-203,000	<i>SPBC660.05</i>	++	-	++
II:221,500-224,000	<i>mik1</i>	+	-	-
II:337,500-340,500	<i>sme2</i>	+	-	-
II:459,500-464,000	<i>SPBC428.10</i>	++++	+	+
II:538,000-541,000	<i>uvi15</i>	+++	+	+
II:919,500-922,500	<i>tor2</i>	+	-	-
II:1,223,500-1,226,000	<i>SPBC725.10</i>	++	-	+
II:1,309,000-1,312,000	<i>soll</i>	+	-	-
II:1,495,000-1,499,000	<i>ivn1</i>	+	-	+
II:2,184,000-2,186,500	<i>cnt5</i>	+++	+	+
II:3,530,000-3,532,500	<i>SPBC1105.13c</i>	++++	++	+++
II:4,103,000-4,108,500	<i>mug147</i>	++	-	+
II:4,409,500-4,414,500	<i>SPBC1289.14</i>	+++	++	+++
III:739,000-742,000	<i>cds1</i>	++	++	++
III:1,265,500-1,268,000	<i>SPCC23B6.01c</i>	+	+	+
III:2,072,000-2,075,000	<i>SPCPB1C11.02</i>	+	+	+
III:2,286,000-2,289,500	<i>yme1</i>	++	+	++
III:2,429,000-2,433,000	<i>SPCC569.03</i>	+++	++	++

*Heterochromatin island numbers correspond to those described previously (Zofall et al., 2012). H3K9-dimethyl (H3K9me2) levels in WT, *swd22Δ* and *ssu72Δ* cells at 18°C were assessed by ChIP-seq. The number of plus signs (+) indicate relative levels of detected H3K9me2. The minus sign (-) denotes a lack of detectable H3K9me2. Genomic coordinates correspond to *S. pombe* genome assembly v2.29. Annotation of Mmi1-dependent and Shelterin-dependent islands was described previously (Zofall et al., 2016; Zofall et al., 2012) Annotation of heterochromatin islands detected at low temperature was described previously (Gallagher et al., 2018).

Table S3. Two categories of Mmi1 regulon genes as defined by H3K9me. Related to Figures 4 and 6.

Mmi1 regulon genes with H3K9me (Islands)

Island number	Gene name
1	<i>mcp7</i>
2	<i>mug8</i>
6	<i>ssm4</i>
8	<i>mcp5</i>
9	<i>mei4</i>
17	<i>mug45</i>
20	<i>mug9</i>

Mmi1 regulon genes without H3K9me (non-islands)

<i>n/a</i>	<i>meu1</i>
<i>n/a</i>	<i>arpl</i>
<i>n/a</i>	<i>tht2</i>
<i>n/a</i>	<i>mug1</i>
<i>n/a</i>	<i>repl</i>
<i>n/a</i>	<i>dli1</i>
<i>n/a</i>	<i>meu43</i>
<i>n/a</i>	<i>mug4</i>
<i>n/a</i>	<i>rec27</i>
<i>n/a</i>	<i>rec25</i>
<i>n/a</i>	<i>spo5</i>
<i>n/a</i>	<i>crs1</i>
<i>n/a</i>	<i>sme2</i>
<i>n/a</i>	<i>dic1</i>
<i>n/a</i>	<i>SPBC1921.04C</i>
<i>n/a</i>	<i>rec10</i>
<i>n/a</i>	<i>rec11</i>
<i>n/a</i>	<i>mug10</i>
<i>n/a</i>	<i>rec8</i>
<i>n/a</i>	<i>mcp6</i>
<i>n/a</i>	<i>meu32</i>

Mmi1 regulon genes as described previously (Chen et al., 2011). Heterochromatin island numbers are same as described previously (Zofall et al., 2012). n/a not applicable.

Table S5. List of oligos used in this study. Related to STAR methods.

Name	Sequence	Purpose
23h314PrmDRv Chk	GGGAAAATCCATAGATTCTGGAAATAGG	ChIP-PCR
ura4termLowChk	CCACAATCTTTTCTCTTGGATTGACATTG	ChIP-PCR
leu1.4	TAGAAGCCTCACCTCCCAA	ChIP-PCR
leu1.3	TTGGTCAAGAGCCCTCGTA	ChIP-PCR
qPCR-leu1-fwd	CCTAAGGAGGCTGAAGCTATCG	qPCR
qPCR-leu1-rev	TCGCGAGTATAAAGACCACGTC	qPCR
Act1 5'ORF FP (VC467)	AAATCGCAGCGTTGGTTATTG	qPCR
Act1 5'ORF RP (VC468)	TTGTCCCATACCTACCATAATACC	qPCR
mei4-qPCR-fwd	CATCGTTCGCACTCAACTGAC	qPCR
mei4-RTPCR-rev	GGTATCTCTCGCGTCGTCAAC	qPCR
ssm4-qPCR-fwd	CAGTTACTAATATCTTCTCAACCTG	qPCR
ssm4-qPCR-rev	GCACTGTTTAACTCGTCTATTAC	qPCR
leu1.1 qPCR Fw	CTGGCAAGGGCATTGTTAAT	qPCR
leu1.2 qPCR Rv	CCACGTCCACCAATTGAAGT	qPCR
ssm4 F	TGTACCGGGAAGTTTGGATTTA	qPCR
ssm4 R	CAACAGTTGCCTTCTTGTCTTC	qPCR
1a11.02 q Fw 2	CGGTCATAAGGATCTTCCTCC	qPCR
1a11.02 q Rv 2	CAGAAGCAATGTGGTACACC	qPCR
428.10 q Fw 2	CTCCCTCTGACGTAAGAGACAAGG	qPCR
428.10 q Rv 2	TCTCTTCCGTAGGTCCGTTAACAG	qPCR
ssm4-3end- qPCR-fwd	GGCTCAAACACAGTTTACGGG	qPCR
ssm4-3end- qPCR-rev	TCCTTGCAGGCAAAGGTCAA	qPCR
KY_dh F	CACCAGACCATTACAAGCAC	qPCR
KY_dh R	TCTCGCCTATTTACCGATCC	qPCR
pho1-2-fwd	GATTTGCTGTTTGGAAAATTAGG	qPCR
pho1-2-rev	CCTGTTGTTCAAACATGTCC	qPCR
nam1-3end- qPCR-fwd	ACGATCCGTCGTGATTGTGT	qPCR
nam1-3end- qPCR-rev	GGTTTCAGAGGACGGCAAGA	qPCR
Ura4 FL F	ATTGCCATACAGTGCCAGGCG	qPCR
Ura4 FL R	TAGCCAAAGAGCCTTTGGAAGAC	qPCR

SPAC23H3.14-qPCR-fwd	GCTGAGCGTCTTGGCAATTT	qPCR (Island 3, H3K9me2)
SPAC23H3.14-qPCR-rev	CGAATGAGCGCTTGGACTTG	qPCR (Island 3, H3K9me2)
ac23H3.14 qPCR Fw1	CGGATTACGGTGAGACATTTCT	qPCR (Island 3, Iss1)
ac23H3.14 qPCR Rv1	TCGCGCAGATATTGGAACCT	qPCR (Island 3, Iss1)
dgT7upfrw	TAATACGACTCACTATAGGCTGCGGTTACCCCTT AAC	Northern blot
dglowrev	CGGATCTAGCTTCGCCATC	Northern blot
byr2_nor_F	CCCAATTTCTCCA ACTTCCA	Northern blot
byr2_nor_R	ATTGTAAGCAATCCGGCAAC	Northern blot
pho1Fwd1	ATTCCTTGGCTTTTTGGCCG	Northern blot
pho1T7Rev2	TAATACGACTCACTATAGGGCTGGGCGGCAGTGT AAATGT	Northern blot